Photogrammetrie • Fernerkundung • Geoinformation 3/2004, S. 215–220, 3 figs.

A Method for Sequential Thinning of Digital Raster Terrain Models

OLGA WÄLDER & MANFRED F. BUCHROITHNER, Dresden

Keywords: digital raster terrain models, DTM, mathematical method for sequential thinning of DTM, wavelet concept

Zusammenfassung: *Ein Verfahren zur sequentiellen Ausdünnung von digitalen Raster Terrain Modellen*. Ein auf Wavelet basierenden Ansätzen beruhendes sequentielles Ausdünnungsverfahren sowie die Beschreibung durch approximierende Funktionen für digitale Raster-Punkt-Geländemodelle wird vorgestellt. Hauptziel ist es, die Struktur des ursprünglichen DGM für weitere Anwendungen bei möglichst geringem Speicheraufwand beizubehalten. Die Qualität dieses sequentiellen Verfahrens kann schrittweise kontrolliert werden. Als Ergebnis dieser Ausdünnung bzw. dieser funktionalen Geländeapproximation wird eine spezielle „Wellen-Struktur" für das reale Georelief erzeugt. Aufbau von Makro- bis Mikrostrukturen des Georeliefs können iterativ verfolgt werden. Das Verfahren wird anhand zweier digitaler Geländemodelle von Testgebieten in den österreichischen Alpen demonstriert. Weitere Möglichkeiten zur Verfeinerung und Verallgemeinerung dieses Ansatzes werden diskutiert.

Summary: A sequential method for the thinning and the description of digital raster terrain models based on wavelet concepts by means of approximating functions is proposed. It aims at the optimum maintenance of the original DTM structure together with a maximum reduction of the memory resources. The sequential thinning quality can be controlled stepwise. As a result of this procedure a special "wave-structure" of the real geo-relief is obtained. The composition of macro- to microstructure of the geo-relief can be followed in an iterative way. The method is demonstrated using the DTMs of two test areas in the Austrian Alps. Further possibilities for the generalization and refinement of this approach are discussed.

1 Motivation and Background

The contributions of the Dresden University of Technology to the scientific programme of the Mars Express Mission (MEX) in 2003/2004 focuses on the development and application of methods and algorithms for the generation of truly three-dimensional hardcopy visualisations based on imagery acquired by the HRSC Mars camera developed at the German Aerospace Center (DLR).

This camera permits improved relief recognition and representation of morphological forms on the Mars surface. Thus, the developed methods and algorithms for the thinning of the relief data need to be tested using simulated as well as real geo-relief data, see WAELDER & BUCHROITHNER (2003).

The generation of an optimized 3D grid based on 3D points from any, not necessarily ordered or complete, data set was presented in a previous publication WAELDER & BUCHROITHNER (2003). As a result of this first step a thinned grid-shaped DGM is obtained. The following step, the thinning and functional approximation of this grid, is described in the present article. This second step can be considered as an independent procedure or as a continuation of the thinning processing described in the above mentioned publication.

1432-8364/04/2004/0215 $ 1.50

The scientific, exciting discussion between LENK and BRIESE & KRAUS (LENK 2003a, b, BRIESE & KRAUS 2003a, b) underlines the topicality of the problem of data simplifications. Obviously, different applications require various assumptions. The present use of wavelets for memory reduction and DTM thinning has been triggered by the work of MEIER (2003). He published some statistical results in the context of compression procedures on the basis of the Wavelet Theory.

In particular, a functional relief approximation allows the sparse data management for their further analysis (deformation tensor determinition, for example) especially for anisotropis cases. Such determinations require differentiations of higher order of the surface equations. Here, the algebraic instead of the numerical differentiation could be used, because the numerical methods show the well-known boundary-effects. So far, the curvature analysis is not considered in our approach.

In contrast to classical wavelet-transformations there are no numerical difficulties caused through the inversion of large matrices. Furthermore, the transition from very fine to coarser approximating structures is possible without any computational effort. The sequentially calculated and locally adapted surface equation is more accurate than global approximations with comparable number of coefficients.

2 Modelling

A grid-formed DTM can be defined by ($\underline{X}$, $\underline{Y}$, $\underline{Z}$) with the matrices $m \times n$

$$\underline{X} = \begin{bmatrix} x_1 & x_2 & \dots & x_n \\ x_1 & x_2 & \dots & x_n \\ \dots & & & \\ x_1 & x_2 & \dots & x_n \end{bmatrix}, \quad \underline{Y} = \begin{bmatrix} y_1 & y_1 & \dots & y_1 \\ y_2 & y_2 & \dots & y_2 \\ \dots & & & \\ y_m & y_m & \dots & y_m \end{bmatrix}$$

and

$$\underline{Z} = \begin{bmatrix} z(x_1, y_1) & z(x_2, y_1) & \dots & z(x_n, y_1) \\ z(x_1, y_2) & z(x_2, y_2) & \dots & z(x_n, y_2) \\ & \dots & & \\ z(x_1, y_m) & z(x_2, y_m) & \dots & z(x_n, y_m) \end{bmatrix}. \quad (1)$$

Out of this data set a new quadratic grid with the number N of rows and columns can be chosen based on m rows and n columns from (1) as follows:

$$N = 2^k + 1 \quad \text{with} \quad k = \log_2 \{\min(n, m)\} \quad (2)$$

Without restriction of general validity, only for the sake of simplification of the presentation, it will be further assumed, that

$$x_i \in [0, 1] \quad \text{for} \quad i = 1, \dots, N \quad \text{and}$$
$$y_j \in [0, 1] \quad \text{for} \quad j = 1, \dots, N:$$

$$x_i = \frac{i-1}{2^k}, \quad y_j = \frac{j-1}{2^k}, \quad z(x_i, y_j) = \underline{Z}(j, i). \quad (3)$$

For the generalised cases the re-scaling or retransformation (x_{gen}, y_{gen}) of (x ,y)–coordinates is given by:

$$x_{(0,1)} = \frac{x_{gen} - \min(x)}{\max(x) - \min(x)},$$
$$y_{(0,1)} = \frac{y_{gen} - \min(y)}{\max(y) - \min(y)},$$
$$x_{gen} = (\max(x) - \min(x)) \cdot x_{(0,1)} + \min(x),$$
$$y_{gen} = (\max(y) - \min(y)) \cdot y_{(0,1)} + \min(y). \quad (4)$$

Finally, it is assumed, that the unknown function $z = z(x, y)\ \forall (x, y) \in R^2$ allows the following approximation $z(x, y) = P_k(x, y)$, $k = 1, 2, \dots$ (c.f. MEIER 2003 and FARIN 1994). Its values are only known at the points (x_i, y_j), $i, j = 1, \dots, N$.

$$P_1(x, y) = a_0 + a_1 \sin(\pi x/2) + b_1 \sin(\pi y/2) + c_1 \sin(\pi x/2) \sin(\pi y/2),$$

$$P_2(x, y) = P_1(x, y) + a_2^{x,y} \sin(\pi x) + b_2^{x,y} \sin(\pi y) + c_2^{x,y} \sin(\pi x) \sin(\pi y),$$

$$P_3(x, y) = P_2(x, y) + a_3^{x,y} \sin(2\pi x) + b_3^{x,y} \sin(2\pi y) + c_3^{x,y} \sin(2\pi x) \sin(2\pi y),$$

$$P_k(x,y) = a_0 + a_1\sin(\pi x/2) + b_1\sin(\pi y/2) + c_1\sin(\pi x/2)\sin(\pi y/2) + a_2^{x,y}\sin(\pi x) + b_2^{x,y}\sin(\pi y) + c_2^{x,y}\sin(\pi x)\sin(\pi y) + a_3^{x,y}\sin(2\pi x) + b_3^{x,y}\sin(2\pi y) + c_3^{x,y}\sin(2\pi x)\sin(2\pi y) + \dots + a_k^{x,y}\sin(2^{k-2}\pi x) + b_k^{x,y}\sin(2^{k-2}\pi y) + c_k^{x,y}\sin(2^{k-2}\pi x)\sin(2^{k-2}\pi y),\quad k = 4,5,\dots \tag{5}$$

The coefficients a, b, c are individual constants for each cell. Because of this, they are marked in (5) with the top indices x, y. This means, that they can vary for different cells. In the following, the calculation and the quality measure of the k$^{\text{th}}$ approximation are discussed.

At first, the expression (5) will be in more detail explained by Fig. 1. For k = 1 there are four corner-points of the 1-cell, which are used for the calculation. So, the coefficients a_0, a_1, b_1, c_1 can be obtained according to (6). Obviously, the other coefficients in (5) are in this case multiplied by zero.

$$\begin{bmatrix} a_0 \\ a_1 \\ b_1 \\ c_1 \end{bmatrix} = \begin{bmatrix} 1 & 0 & 0 & 0 \\ 1 & 1 & 0 & 0 \\ 1 & 0 & 1 & 0 \\ 1 & 1 & 1 & 1 \end{bmatrix}^{-1} \begin{bmatrix} z(0,0) \\ z(1,0) \\ z(0,1) \\ z(1,1) \end{bmatrix}. \tag{6}$$

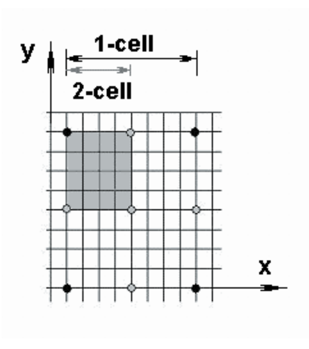

Fig. 1: Grid modelling. The four black points are chosen by the first approximation step (1-cell). The five additional grey points go into the second approximation step (2-cell).

The precision of the 1-approximation can be estimated by (7):

$$G_1 = \frac{1}{N^2}\sum_{i,j=1}^{N} |z(x_i, y_j) - P_1(x_i, y_j)| \tag{7}$$

In a next step, the 1-cell will be divided into four parts. These parts are called 2-cells. For each 2-cell the new coefficients a_2, b_2, c_2 are calculated. For example, for the left-top 2-cell with coordinates at its bottom left corner equalling to (0, 0.5) this leads to:

$$\begin{bmatrix} a_2^{0,0.5} \\ b_2^{0,0.5} \\ c_2^{0,0.5} \end{bmatrix} = \begin{bmatrix} 0 & 1 & 0 \\ 1 & 1 & 1 \\ 1 & 0 & 0 \end{bmatrix}^{-1} \cdot \begin{bmatrix} z(0,0.5) - P_1(0,0.5) \\ z(0.5,0.5) - P_1(0.5,0.5) \\ z(0.5,1) - P_1(0.5,0) \end{bmatrix}. \tag{8}$$

For the other three 2-cells the calculation is the same. It shall just be mentioned once again, that all coefficients a_j, b_j, c_j for $j > 2$ from (5) are multiplied by zero.

The quality of the second approximation step can be estimated according to (7):

$$G_2 = \frac{1}{N^2}\sum_{i,j=1}^{N} |z(x_i, y_j) - P_2(x_i, y_j)| \tag{9}$$

This method can be continued until the apriori defined accuracy will be achieved. Thus, the l^{th} approximation step for the left-top l-cell reads:

$$\begin{bmatrix} a_l^{0,1-\frac{1}{2^{l-1}}} \\ b_l^{0,1-\frac{1}{2^{l-1}}} \\ c_l^{0,1-\frac{1}{2^{l-1}}} \end{bmatrix} = \begin{bmatrix} 0 & 1 & 0 \\ 1 & 1 & 1 \\ 1 & 0 & 0 \end{bmatrix}^{-1} \cdot \begin{bmatrix} z\left(0, 1-\frac{1}{2^{l-1}}\right) - P_{l-1}\left(0, 1-\frac{1}{2^{l-1}}\right) \\ z\left(\frac{1}{2^{l-1}}, 1-\frac{1}{2^{l-1}}\right) - P_{l-1}\left(\frac{1}{2^{l-1}}, 1-\frac{1}{2^{l-1}}\right) \\ z\left(\frac{1}{2^{l-1}}, 1\right) - P_{l-1}\left(\frac{1}{2^{l-1}}, 1\right) \end{bmatrix}$$

and

$$G_l = \frac{1}{N^2}\sum_{i,j=1}^{N} |z(x_i, y_j) - P_l(x_i, y_j)|. \tag{10}$$

Hence, the approximation used here is a sequential, continuous and differentiable spline approximation by sine-like wavelets.

3 Case Study Austrian Alps (Granatspitz Massif)

In 1999 a large area in the Austrian Hohen Tauern, southwest of Zell am See, was remotely sensed by the HMRSC camera developed by the German Aerospace Center (DLR). This high-alpine area reaches from approx. 800 m to 3150 m a.s.l. It is characterized by a richness in geomorphological forms and therefore perfectly suitable as a test area.

In order to illustrate the method described above, a grid DTM with approx. 100×100 points is thinned into a 5×5 grid by three

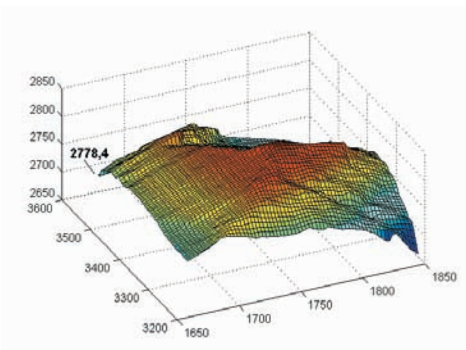

Fig. 2a: Original raster DTM of approx. 10.000 points.

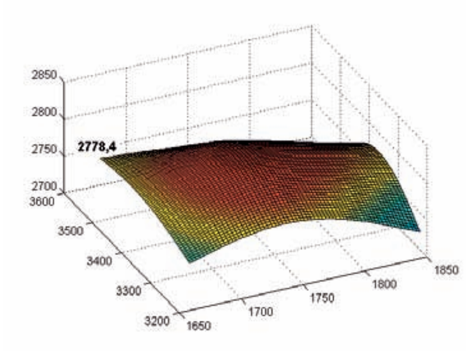

Fig. 2b: Second approximation step: out of 10.000 points only 9 points and $4 + 4 \times 3 = 16$ coefficients remain. Here sine-like wavelets were used.

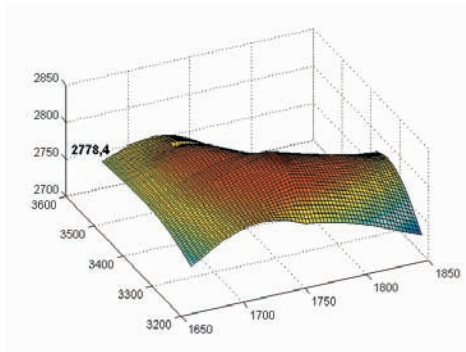

Fig. 2c: Third approximation step: out of 10.000 points only 25 points and $4 + 4 \times 3 + 16 \times 3 = 64$ coefficients remain. Here sine-like wavelets were used.

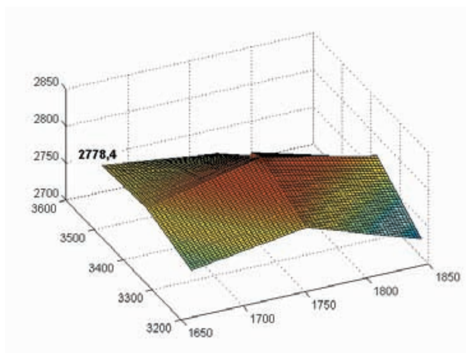

Fig. 2d: Second approximation step: out of 10.000 points only 9 points and $4 + 4 \times 3 = 16$ coefficients remain. Here zigzag-shaped wavelets were used.

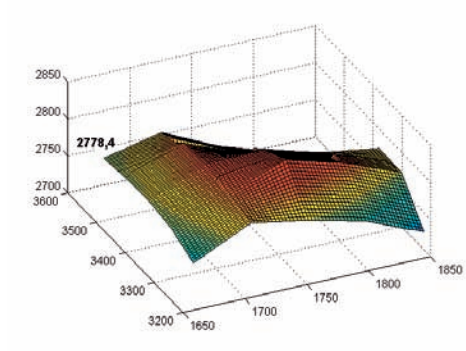

Fig. 2e: Third approximation step: out of 10.000 points only 25 points and $4 + 4 \times 3 + 16 \times 3 = 64$ coefficients remain. Here zigzag-shaped wavelets were used.

approximation steps (see Fig. 2a–c). The accuracies thereby obtained are by using *sine-like* wavelets (in [m]):

$$G_1 = 45.94\,,\quad G_2 = 10.28\,,\quad G_3 = 3.08\,. \qquad (11)$$

The accuracies are obtained by using *zigzag-shaped* wavelets (in [m]) for the same data set, Fig. 2d–e:

$$G_1 = 39.20\,,\quad G_2 = 13.70\,,\quad G_3 = 3.63\,. \qquad (11a)$$

Generally, the first step is never sufficient. The second step results in a 3×3 grid, which, on the basis of 9 points (of 10.000 in the original DTM!), respects the macrostructure of the relief. Starting with the 5×5 grid, this structure is continued to be further refined. So, we need to save the number of steps equal 3 here, four original x, y-coordinates of edge grid points and $1 \times 4 + 4 \times 3 + 16 \times 3 = 64$ coefficients instead of 10.000 z-coordinates + 4×2 x, y-coordinates of edge grid points + length N of the original quadratic grid. Less than 0.73 % of the original data remain after thinning.

It has to be noted that not only sinusoidal wavelets can be used in expression (5). Fig. 3a presents another alpine test area with approx. 60.000 points. Fig. 3b shows the 4-step spline-approximation with 81 points and with *sine-like* wavelets. The accuracies thereby obtained are (in [m]):

$$G_1 = 20.24\,,\quad G_2 = 12.37\,,\quad G_3 = 8.50\,,\quad G_4 = 5.39\,. \qquad (12)$$

Here, less than 0.45 % of the original paster data are remained after thinning (number of steps, four edge grid points and $1 \times 4 + 4 \times 3 + 16 \times 3 + 64 \times 3 = 256$ coefficients instead of 60.000 z-coordinates + 4×2 x, y-coordinates of edge grid points + length N of the original quadratic grid). Fig. 3c presents the 4-step approximation with the same number of points and with *zigzag-shaped* wavelets.

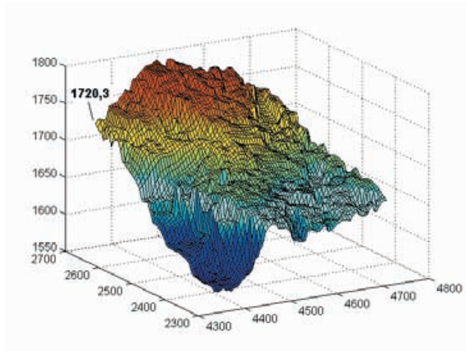

Fig. 3a: Original raster DTM of ca. 60.000 points.

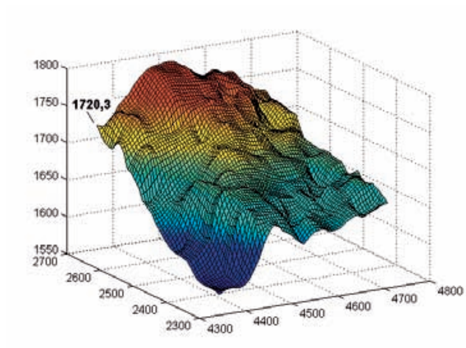

Fig. 3b: 4th approximation step: first, the grid structure is maintained. Out of ca. 60.000 points only 81 and 256 coefficients remain. Here sine-like wavelets were used.

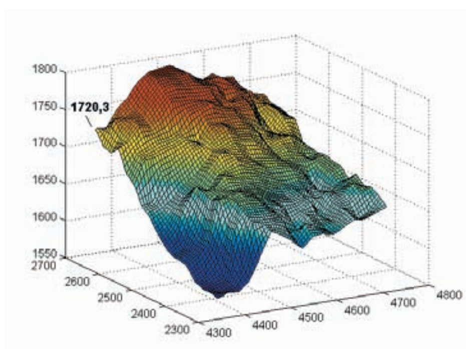

Fig. 3c: 4th approximation step: first, the grid structure is maintained. Out of ca. 60.000 points only 81 and 256 coefficients remain. Here the zigzag-shaped wavelets were used.

The corresponding accuracies obtained for Fig. 3a are (in [m]):

$$\begin{aligned} G_1 &= 25.42\,,\\ G_2 &= 13.64\,,\\ G_3 &= 8.33\,,\\ G_4 &= 5.24\,. \end{aligned} \qquad (12a)$$

The approximation in Fig. 3c is less smoothed than the one in Fig. 3b. Thus, it seems to be more suitable for a pronounced relief. Moreover, any combination of both of these two approximations is possible. The comparison of (12) and (12a) allows to set the hypothesis, that a certain approximations level (or step) could exist, which depends on geomorphologic structures of relief and presents a limit for the transition from sine-like to zigzag wavelets. It can be seen from (12), that the sine-like wavelets are more suitable as zigzag here. Until the 3^{th} step the accuracies by using zigzag-shaped wavelets are lower than they by using sine-like wavelets.

4 Outlook

The presented approach has been implemented in our Windows-based in-house software tool DEFAN. It needs, however, to be both generalized and refined. In a first step, additional information in the form of breaklines will be considered. Further, the performance of combined, sine-like and zigzag-shaped wavelet models will to be investigated. Their approximation accuracy will help to answer the question to what extent the resulting macro- and micro-structures correspond to their real-world geomorphological equivalents. In this respect, the role of relief-energy presentations in determing the optimal modelling approach also needs to be exploited.

Acknowledgements

The present article has been prepared within the scope of the Mars Express Project (MEX) with financial support of the German Aerospace Center (DLR) and the BMBF at the Institute for Cartography of the Dresden University of Technology. We wish to thank two anonymous reviewers for their constructive comments which significantly helped to improve the quality of this paper.

References

Briese, Ch. & Kraus, K., 2003a: Datenreduktion dichter Laser-Geländemodelle. – ZfV, 2003/5: 312–317.

Briese, Ch. & Kraus, K., 2003b: Stellungnahme zu „2.5D-Diskontinuitäteten in der Geländemodellierung und spezielle Aspekte bei Delaunay-Triangulationen". – ZfV, 2003/6: 366.

Farin, G., 1994: Kurven und Flächen in Computer Aided Geometric Design: Eine praktische Einführung. – Vieweg Publishers, Braunschweig/Wiesbaden.

Lenk, U., 2003a: Triangulation und Adaptive Triangulationen – ein Verfahren zur Ausdünnung unregelmäßig verteilter Massenpunkte in der Geländemodellierung. – ZfV, 2003/1:47–56.

Lenk, U., 2003b: 2.5D-Diskontinuitäten in der Geländemodellierung und spezielle Aspekte bei Delaunay-Triangulationen. – ZfV, 2003/6: 357–365.

Meier, S., 2003: Zur K-Frage: Kompressionsraten der schnellen Wavelettransformation aus statistischer Sicht. – ZfV, Sonderdruck, 2003/1: 31–40.

Wälder, O. & Buchroithner, M. F., 2003: Eine Anwendung von Spline-Verfahren zur DTM-Ausdünnung. – PFG, 2003 (2): 99–104.

Addresses of the authors:

Dr. rer. nat. Olga Wälder,
Prof. Dr. phil. habil. Manfred Buchroithner
Institute for Cartography
Dresden University of Technology
Mommsenstrasse 13, D-01062 Dresden
Tel.: 0351-4633-6200 or 0351-4633-4809
Fax: 0351-4633-7028
e-mail-Adressen:
Olga.Waelder@mailbox.tu-dresden.de
Manfred.Buchroithner@mailbox.tu-dresden.de

Manuskript eingereicht: November 2003
Angenommen: Februar 2004